R. & M. No. 2979
(17,442)
A.R.C. Technical Report

MINISTRY OF SUPPLY

AERONAUTICAL RESEARCH COUNCIL
REPORTS AND MEMORANDA



# The Secondary Flow in a Cascade of Turbine Blades

*By*

W. D. ARMSTRONG



LONDON : HER MAJESTY'S STATIONERY OFFICE
1957
PRICE 4s 6d NET

# The Secondary Flow in a Cascade of Turbine Blades

*By*

W. D. ARMSTRONG

Department of Engineering, University of Cambridge

COMMUNICATED BY THE PRINCIPAL DIRECTOR OF SCIENTIFIC RESEARCH (AIR), MINISTRY OF SUPPLY

*Reports and Memoranda No.* 2979

*March,* 1955

*Introduction.*—In recent papers it has been demonstrated that the so-called secondary flow which occurs when a non-uniform stream passes through a cascade of turning vanes or blades can be calculated by a consideration of the turning of the vorticity vectors. Whenever the upstream vorticity or the angle of turn is small the perturbation method of Squire and Winter[1] or Hawthorne[2] may be used for the calculation of the downstream vorticity component in the stream direction between the blades. Estimation of the induced velocities however requires a knowledge of the flow which would exist in the absence of the streamwise vorticity. It has been shown[3] that this flow is not normally two-dimensional but may be calculated by an analytical technique whereby the cascade of blades is replaced by an ' actuator plane.' In certain special cases this basic flow is two-dimensional and can be used to demonstrate the applicability of the simple perturbation secondary flow theories.

Many practical examples of secondary flow involve conditions which are beyond the limits of the perturbation theories and then an initial experimental approach to the problem enables suggestions to be made for the simplification of the analytical difficulties.

*Impulse Turbine Cascade.*—By using the concept of an actuator plane to replace a cascade of blades an approximate expression has been derived in a previous paper[3] for the variation of air angle far downstream of the cascade. In the special case when $\alpha_1 = -\alpha_2$ the change of angle in a downstream plane is solely due to the distributed vorticity within the blade passages, since the flow in the absence of this vorticity is purely two-dimensional and there is no displacement effect such as is calculated in Ref. 3.

Experiments made with $\alpha_1 \simeq -\alpha_2$ will therefore display primarily the effects of a secondary distributed vorticity superimposed on a two-dimensional motion. Since it has been shown[4] that downstream of the trailing edge the blade wakes act as continuations of the blade surfaces, observations of the ' rolling up ' of the secondary flow may be made.

*Experiments.*—For this investigation a cascade of ' impulse ' turbine blades was used in a 150 h.p. pressure wind tunnel. Nine 6-in. chord blades were used with a blade spacing of 6 in., the aspect ratio being 3. The blade shape shown in Fig. 1 is one constructed entirely of straight lines and circular arcs. To provide a slight pressure drop through the blading, thereby obviating extensive secondary stalling, the blades were set at a stagger angle of + 10 deg and air inlet angle, $\alpha_1$ of 35 deg. The design outlet angle was 37 deg.

Two groups of tests were made, one using an artificially thickened wall boundary layer (Fig. 2) to give a low upstream vorticity and in the second the two natural boundary layers formed on the tunnel walls perpendicular to the blade length constituted the non-uniformity (Fig. 3). The natural boundary layers have the usual turbulent form with an overall thickness of about 1 in., leaving a central region of uniform flow 16 in. wide. Measurements were made one chord upstream of the blades and in planes between the trailing edge and a position $1\frac{1}{2}$ chords downstream. In each traverse plane the total head and air angles in two perpendicular planes were determined at approximately 1,100 points over a region two pitches wide and half the blade length long. The experimental results are presented in the form of maps (Figs. 4 to 9).

*Discussion of Results.—Perturbation Tests.*—The incident velocity profile approaching the two centre passages which is shown in Fig. 2 is approximately linear, except close to the tunnel wall where presumably it becomes very steep. The main secondary effects will be created by the linear portion but the part close to the wall will be to some extent effective in rotating the flow. A contour map of total head just downstream of the trailing edges (Fig. 4) demonstrates qualitatively the rotational flow. It can be seen, by comparison with later results (Fig. 6) that the upstream vorticity is sufficiently small for the Bernoulli planes to remain effectively parallel to the walls and therefore for the perturbation theory to be applied directly.

There are two ways in which the theoretical and experimental results may be compared. The measured values of the induced velocities can be differentiated and combined to give the secondary distributed stream vorticity for comparison with the theoretical, $2\varepsilon.dU_1/dZ$, or the measured induced velocities may be compared directly with the calculated values.

Whilst the former method is obviously a more complete correlation there are inherent disadvantages in that both induced velocities must be known accurately everywhere to enable the $\partial V_2/\partial Z$ and $\partial W_2/\partial Y$ components to be determined with any certainty. In these tests as in all experiments made close to the trailing-edge plane, $W_2$ can be determined but the induced velocity $V_2$ is subject to error in some regions. The induced velocity $V_2$ is obtained from the difference between the actual outlet angle and the outlet angle which would have been attained in a perfect two-dimensional flow. It is the two-dimensional angle which is uncertain in a region between the trailing edges and a plane about half a chord downstream. Close to the trailing-edge plane the outlet angle varies considerably between two blades, *i.e.*, across a pitch, even where the flow is basically two-dimensional. At distances greater than about half a chord downstream the two-dimensional angle becomes constant since the potential flow solution has by this time developed its final parallel régime.

The second method, *viz.*, comparison of the induced velocities themselves was therefore adopted.

Taking the measured values of $dU_1/dZ$ in the lower passage, relaxation methods were used to calculate the secondary stream function $\psi$ given by $\nabla^2\psi = 2\varepsilon.dU_1/dZ$. From the gradients of $\psi$ the theoretical values of $W_2$ were calculated. These are shown along with the experimental values of $W_2$ in Fig. 5, the two sets of curves relating to spanwise positions 3 in. and 6 in. from the blade centre-line, *i.e.*, 6 in. and 3 in. from the cascade wall. The latter position corresponds approximately to the point of maximum $\psi$ and therefore maximum induced velocity $W_2$. In general the experimental velocities are in good agreement with those calculated using the perturbation theory. In the region close to the convex surface the apparent discrepancy can be simply explained by inspection of the relevant plot of downstream total head. There it will be seen that at points having low experimental induced velocities the main stream velocity is also very small, in fact these points lie within the boundary layer on the blade convex surface. At this position along the span (3 in. from the wall) the blade boundary layer has attained almost its maximum thickness because of the transport of the cascade wall boundary layer associated with the steep velocity profile close to the wall.

The actual variation in shape of the $W_2$ curve between the mid-pitch point and the concave surface may possibly be due to localised vorticity effects caused by the blade nose shapes or the negative incidence.

*Tests with Considerable Upstream Vorticity.*—The ' natural boundary layer ' inlet velocity profile is shown for half the blade span in Fig. 3. Figs. 6 and 7 show the resulting total head maps in planes $\frac{1}{2}$ and $1\frac{1}{2}$ chords downstream of the trailing edges. Using the angle measurements the corresponding induced velocity components have been calculated and are shown as maps of vectors in Figs. 8 and 9. (Note that in both cases the ordinate is in the tangential or $y$ direction whilst the induced velocity is in the $Y$ direction, *i.e.*, normal to the main flow.) Integrated values of $V_2$ over two blade pitches are plotted along the blade span in Fig. 10 for each of the two downstream planes.

Fig. 10 shows that even with a boundary layer $\frac{1}{9}$th of the half span there are appreciable $V_2$ induced velocities over most of the span. If the flow could have been regarded as a perturbation on a two-dimensional flow, then it would have been possible to calculate the values of the induced velocities. Experience has shown however that the maximum value of the secondary stream function $\psi$ occurs within the boundary layer whereas in this case the zero value of $V_2 = \partial\psi/\partial Z = 0$ occurs at the edge of the upstream boundary layer. In addition study of Figs. 8 and 9 reveals that the $W_2$ velocities are of the same sign across almost the whole of the blade pitch whereas the perturbation theory would indicate a change in the sign of $W_2$ in the inter-wake position.

Superimposition of the total-head map (Fig. 6) and the vector map (Fig. 8) shows that instead of the secondary vorticity being distributed uniformly across the blade passage it is concentrated in a very small region in the corner of the blade passage adjacent to the convex blade surface. This is caused by the very high value of the upstream vorticity $dU_1/dZ$ and therefore large secondary vorticity. As the induced $V_2$ velocity increases through the blade passage so the boundary layer on the wall of the tunnel gradually becomes swept on to the convex surface of the blade. Once a portion of the boundary layer reaches this surface its secondary vorticity remains fixed and no longer increases as the main stream turning continues. A situation arises therefore in which the whole of the air which formerly comprised the upstream boundary layer has been swept on to the blade convex surface, there it remains rotating but not gaining any further secondary vorticity as the main stream deflection increases.

An approximate calculation of the strength of the secondary circulation under these circumstances (*see* Appendix) shows that the whole of the wall boundary layer would be transported onto the blade after an angle of turn of about 40 deg compared with the main stream turning of 72 deg. This figure agrees well with the flow observed near the wall. Tufts of goosedown attached to the wall are shown in Fig. 11 and from these the path of the air from the leading edge to the convex surface may be followed.

The pattern of the flow between planes $\frac{1}{2}$ chord and $1\frac{1}{2}$ chords downstream of the blades may be followed by comparing Figs. 6 and 8 with Figs. 7 and 9. It is found that the air stream continues to rotate, principally in the direction of the secondary vorticity so that it collects together in its vortex core all the air having the lowest total head. The velocities are such that the wake tends to be cut, leaving a rotating region which gradually moves away from the wall and the central region which bends slowly as it moves downstream.

This then is the type of flow observed when the initial vorticity $dU_1/dZ$ is so great and the secondary vorticity so concentrated that the induced secondary effects themselves become important in calculating the distributed secondary vorticity.

*Conclusion.*—It has been shown that when the secondary vorticity is sufficiently small the perturbation theory of Refs. 1 and 2 may be used to predict accurately the induced velocities downstream of the blades which are due to this distributed vorticity. As the upstream vorticity or the blade deflection is increased then the perturbation theory is no longer applicable and the

transport of the Bernoulli surfaces within the blade passages must be considered. In a particular case a crude approximate method has been given for the calculation of the distributed circulation but this itself does not enable the induced velocities to be computed.

Experimental evidence is presented to show that downstream of the cascade there are, for each blade, two adjacent regions of low total head which rotate in opposite directions. One of these regions originates from the blade shed circulation and the other from the distributed secondary circulation within the blade passage.

## REFERENCES


| *No.* | *Author* | *Title, etc.* |
|---|---|---|
| 1 | H. B. Squire and K. G. Winter .. .. | The secondary flow in a cascade of aerofoils in a non-uniform stream. *J. Ae. Sci.* Vol. 18, p. 271. 1951. |
| 2 | W. R. Hawthorne .. .. .. .. | Secondary circulation in fluid flow. *Proc. Roy. Soc. A.* Vol. 206, p. 374. 1951. |
| 3 | W. R. Hawthorne and W. D. Armstrong | Shear flow through a cascade. *Aero. Quart.* Vol. VII, p. 247. 1956. |
| 4 | W. R. Hawthorne and W. D. Armstrong | Rotational flow through cascades. Part II : The circulation about the cascade. *Quart. J. Mech. App. Maths.* Vol. 8, p. 288. 1955. |


## APPENDIX

*An approximate calculation of the secondary passage circulation used when the induced velocities are large*

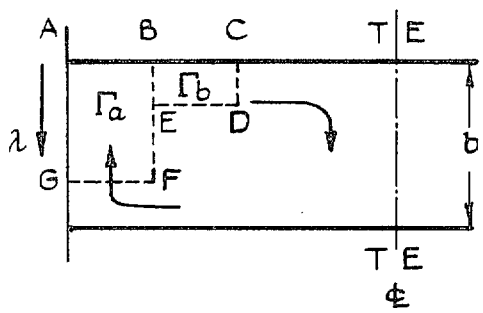


The figure shows very crudely the position of the wall boundary layer after an angle of turn $\theta$. At this point let the circulation within the boundary layer now on the blade be $\Gamma_b$ and that for the boundary layer still attached to the wall be $\Gamma_a$. Then if $\lambda$ is the length of wall boundary layer $\Gamma_a = 2U\lambda\theta$ where $U$ is the main stream velocity which for the turbine impulse blade considered here is constant.

The net circulation $\Gamma = \Gamma_b + 2U\lambda\theta$.

After a further small turn $d\theta$ the net circulation is

$$\Gamma + d\Gamma = 2(\lambda - d\lambda)U(\theta + d\theta) + 2U\theta\, d\lambda + \Gamma_b$$

since there is no increment of circulation for the fluid which now lies along the blade.

Subtracting, $d\Gamma = 2U\lambda\, d\theta$.

To integrate this expression it is necessary to calculate $\lambda$.

If $v$ is the velocity of the boundary layer up the side wall then $d\lambda = -v\,dt = -vR\,d\theta/U$ where $R$ is the radius of curvature of the blade passage.

Experimental evidence shows that :

(*a*) the induced velocity of the main stream edge of the boundary layer is very small compared with the wall edge

(*b*) the fluid which has passed from the wall onto the blade surface does not go rapidly along the blade but because of the high energy air coming over the blade surface it collects as an increasingly large pocket of stagnant air.

Take a path round ABCDEFG—the only important velocity component round the border is $v$.

Therefore $\Gamma = v\lambda = \Gamma_b + \Gamma_a$

or $v = \Gamma/\lambda$.

With no movement on to the blade surface the net circulation after a deflection $\theta$ would be given by $\Gamma = 2b\theta U$ where $b = \sigma \cos \alpha_2$.

As a first approximation take $\Gamma = 2Bb\theta U$ where $B < 1$.

Then $d\lambda = -vR\,d\theta/U$

$$\lambda\,d\lambda = -2RbB\theta\,d\theta,$$

*i.e.*, $\lambda^2 = b^2 - 2RbB\theta^2$.

Therefore $\lambda = 0$, *i.e.*, all the boundary layer is on the blade surface when

$$\theta^2 = \frac{b}{2RB} \quad \text{or} \quad \theta = \left[\frac{b}{2RB}\right]^{1/2}.$$

$$d\Gamma = 2U\lambda\,d\theta$$

$$= 2U(b^2 - 2RbB\theta^2)^{1/2}\,d\theta$$

$$\Gamma = \frac{2Ub}{\sqrt{(b/2RB)}}\left[\frac{b}{4RB}\sin^{-1}\frac{\theta}{\sqrt{(b/2RB)}} + \theta\sqrt{(b/2RB - \theta^2)}\right]_{\theta = 0}^{\theta = \sqrt{(b/2RB)}}$$

$$= \frac{\pi Ub}{2}\sqrt{\left(\frac{b}{2RB}\right)}.$$

Unless fresh boundary layer is created there is no further increase in circulation for values of $\theta > \sqrt{(b/2RB)}$.

In the turbine blade experiments $b = 4{\cdot}8$ in., $R = 5{\cdot}3$ in. approximately, and if $B = 1$, $\theta = 39$ deg at the point at which all the boundary layer has moved on to the blade surface and the net circulation $\Gamma = 5{\cdot}07U$—compare with goosedown on Fig. 11.

If there had been the full secondary circulation $\Gamma$ would have been $12{\cdot}0U$, or $6{\cdot}50U$ for only 39 deg deflection ; therefore an improved value of $2B$ would be $1{\cdot}57$.

This gives $\theta = \sqrt{(b/2RB)} = 43{\cdot}5$ deg and $\Gamma = 5{\cdot}73U$.

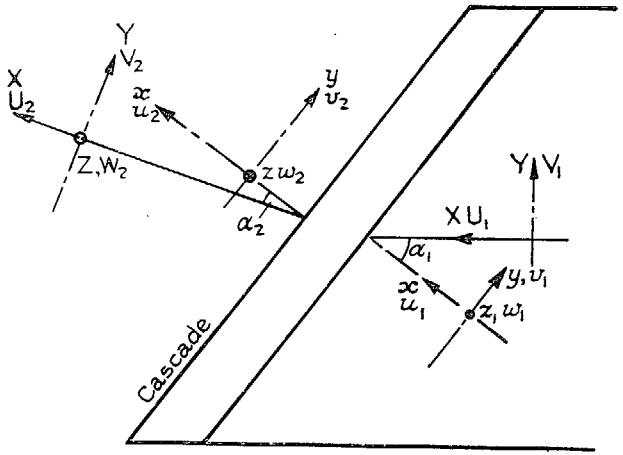


Co-ordinate system.

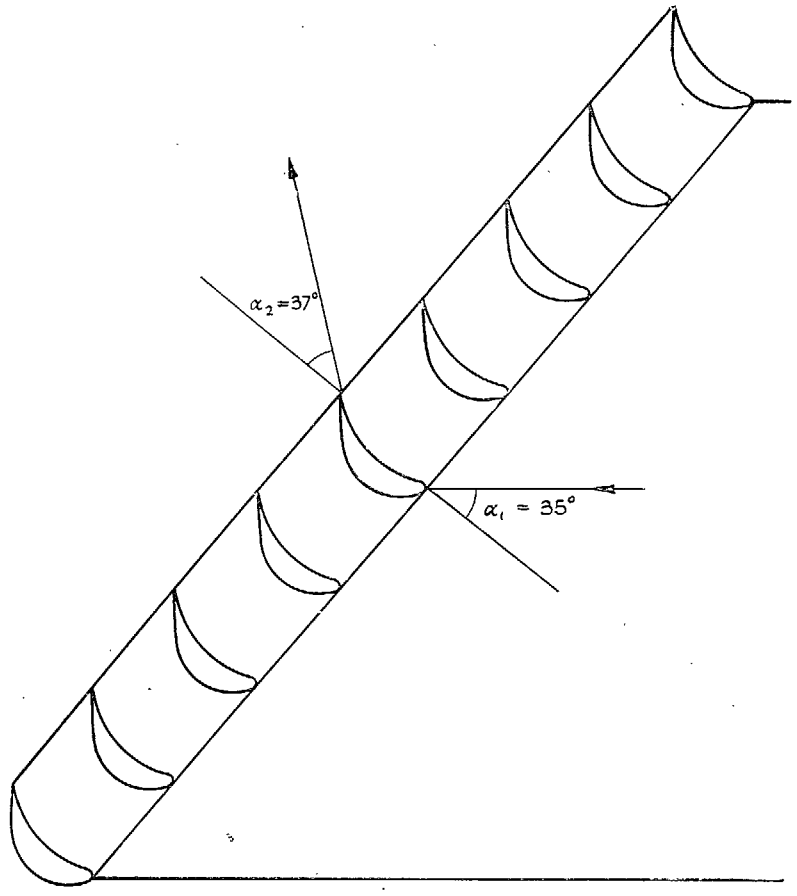


Scale:- 0 6″ 12″

Chord 6″ pitch 6″ span 18″ $\zeta = +10°$

**Notation**

| | |
|---|---|
| $x, y, z$ | Axial, tangential and blade spanwise coordinates |
| $u, v, w$ | Axial, tangential and blade spanwise velocity components |
| X, Y, Z | Coordinate system relative to X as main stream direction |
| U, V, W | Velocity components in X Y Z directions |
| $\alpha$ | Air angle measured from perpendicular to cascade |
| $\epsilon$ | Air deflection |
| $\psi$ | Stream function |

**Subscripts**

| | |
|---|---|
| 1 | Far upstream |
| 2 | Far downstream |

FIG. 1. Turbine cascade.

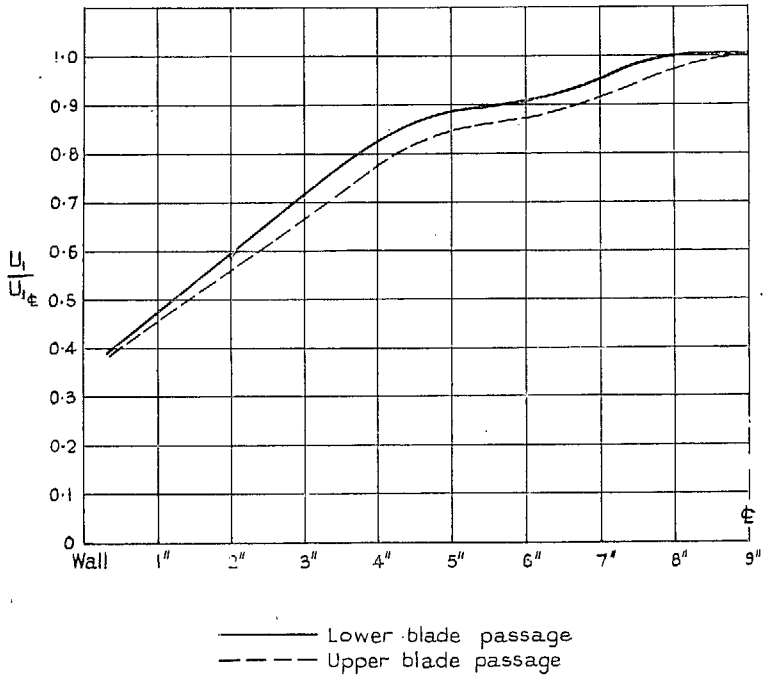


FIG. 2. Inlet velocity profile. Artificially thickened boundary layer.

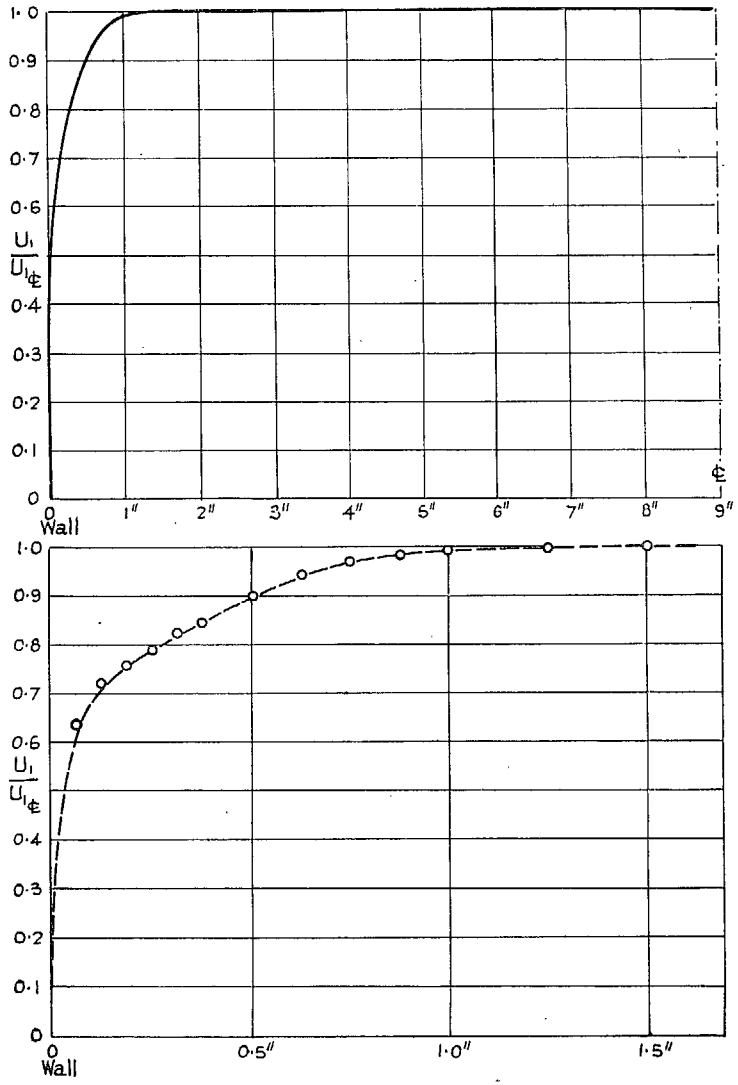


FIG. 3. Inlet velocity profile. Thin boundary layer.

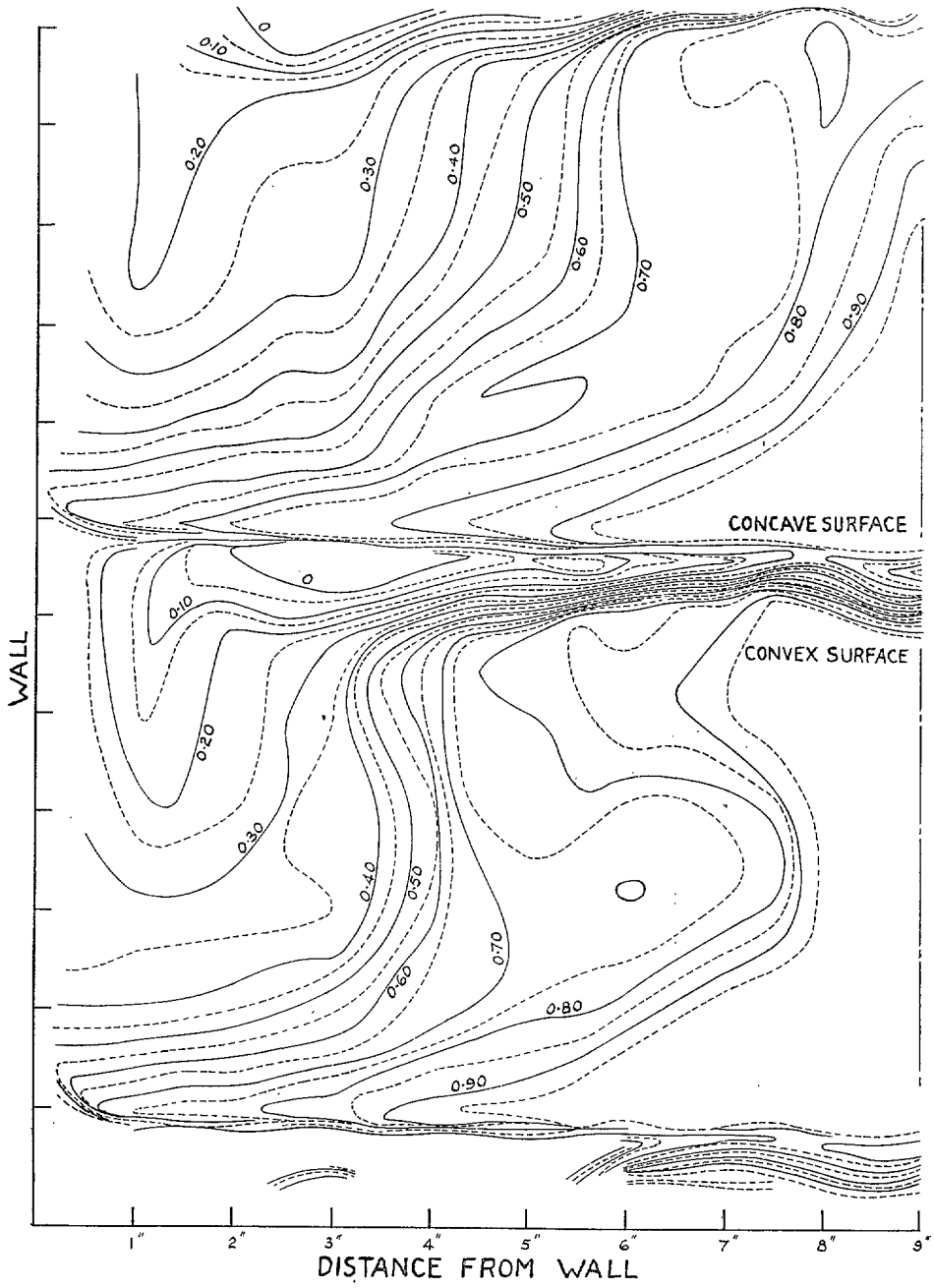


FIG. 4. Contours of constant total head in the trailing-edge plane.
Thick boundary layer.

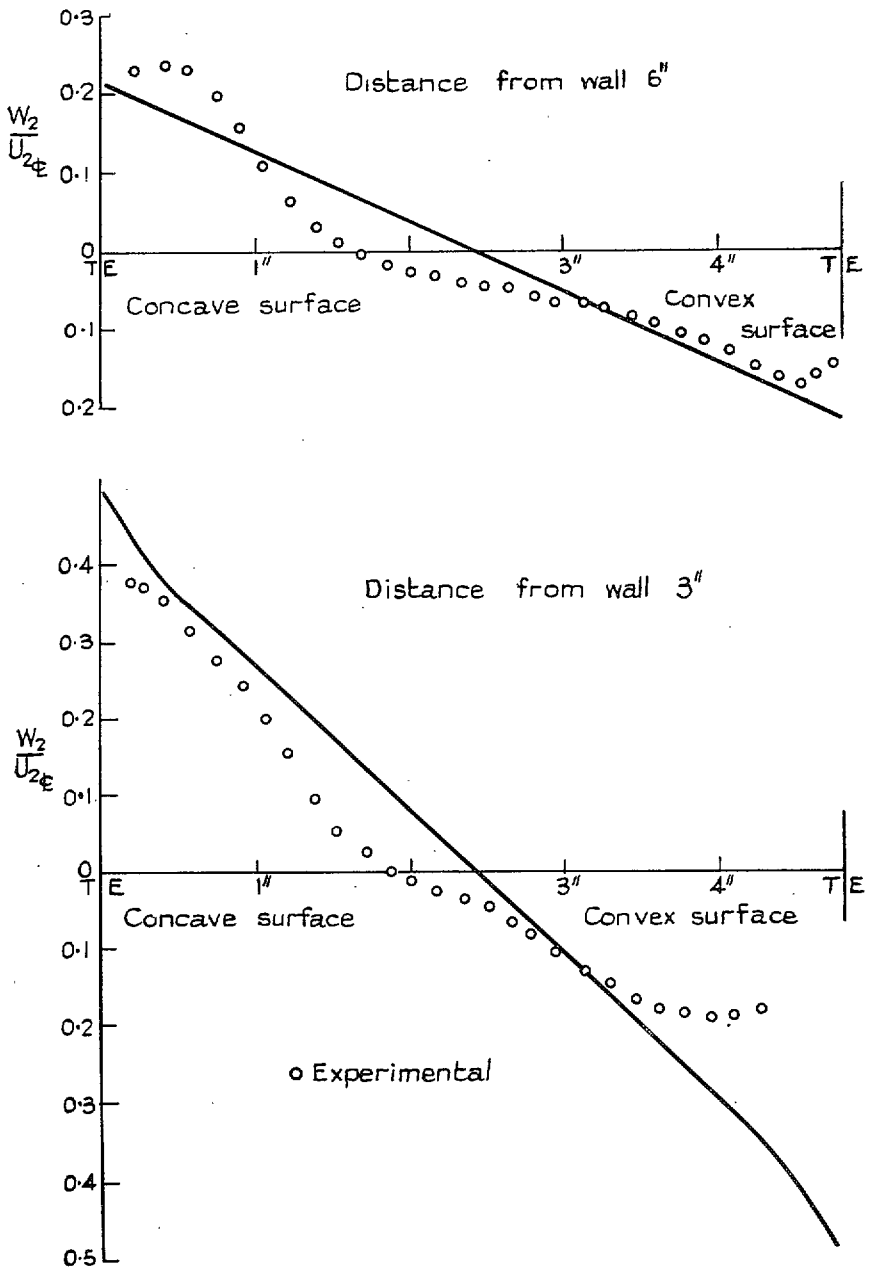


FIG. 5. Induced spanwise velocity $W_2$. Thick boundary layer.

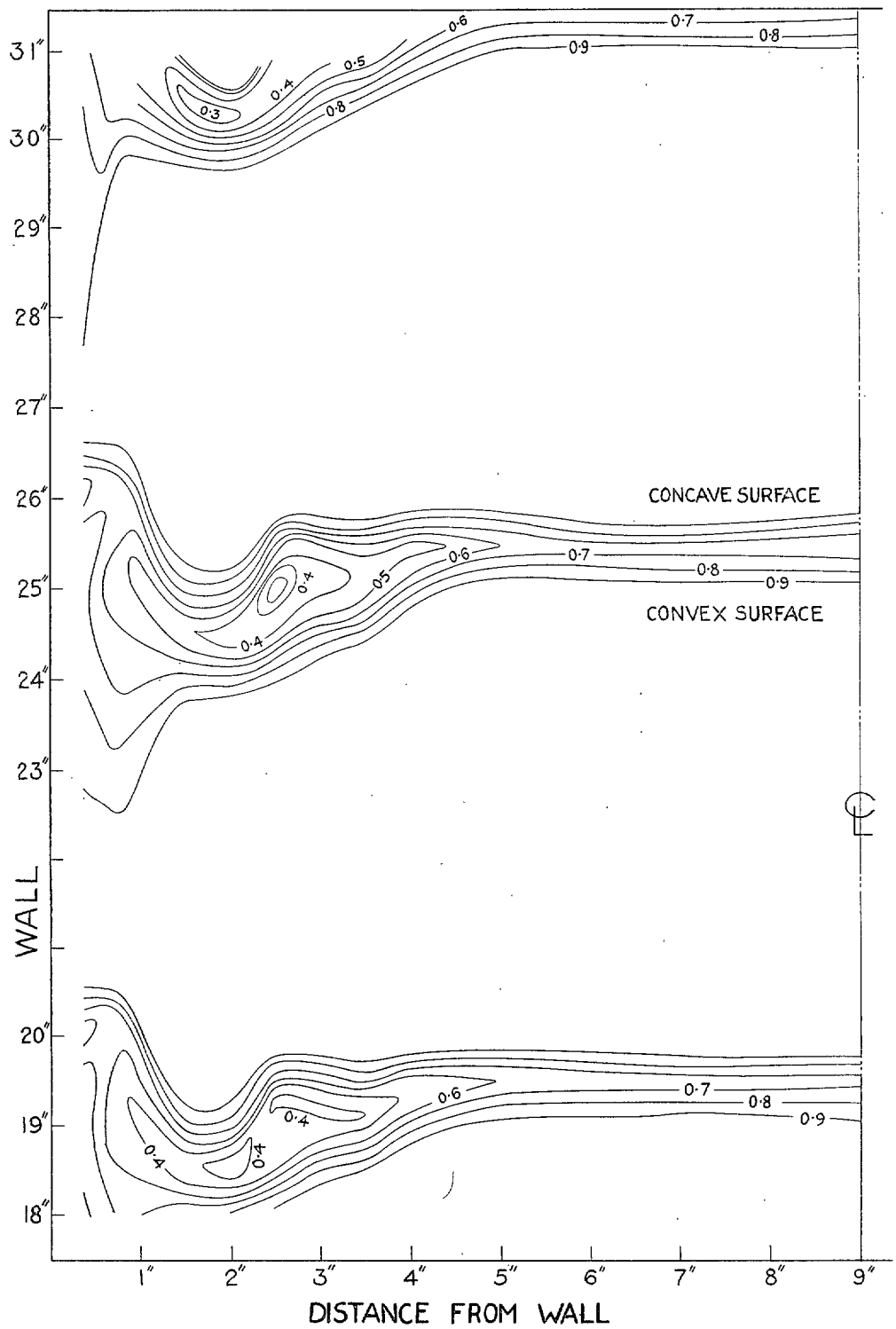


FIG. 6. Contours of constant total head in a plane $\frac{1}{2}$ chord downstream of the trailing edge. Thin upstream boundary layer.

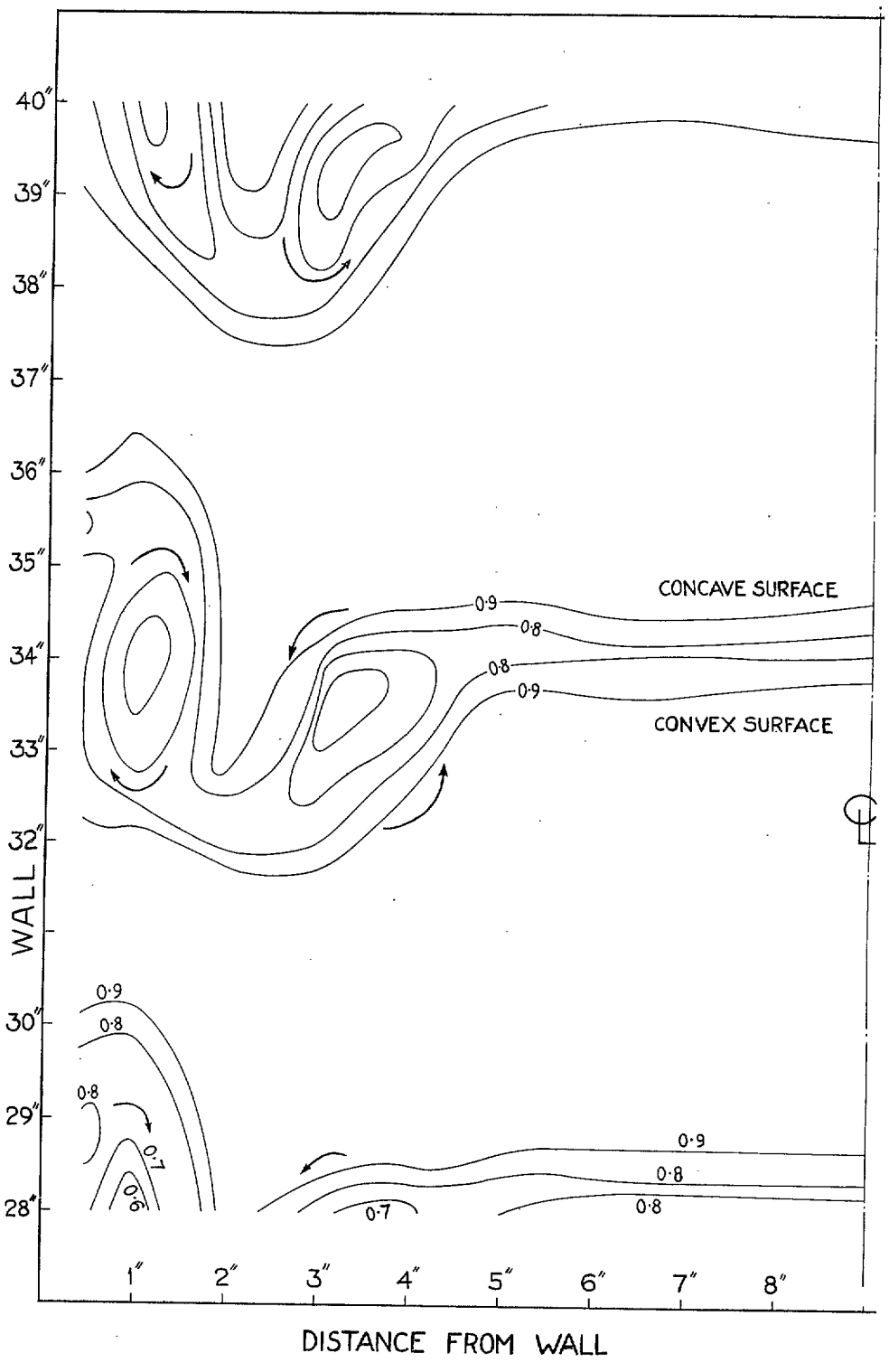


FIG. 7. Contours of constant total head in a plane $1\frac{1}{2}$ chords downstream of the trailing edge. Thin upstream boundary layer.

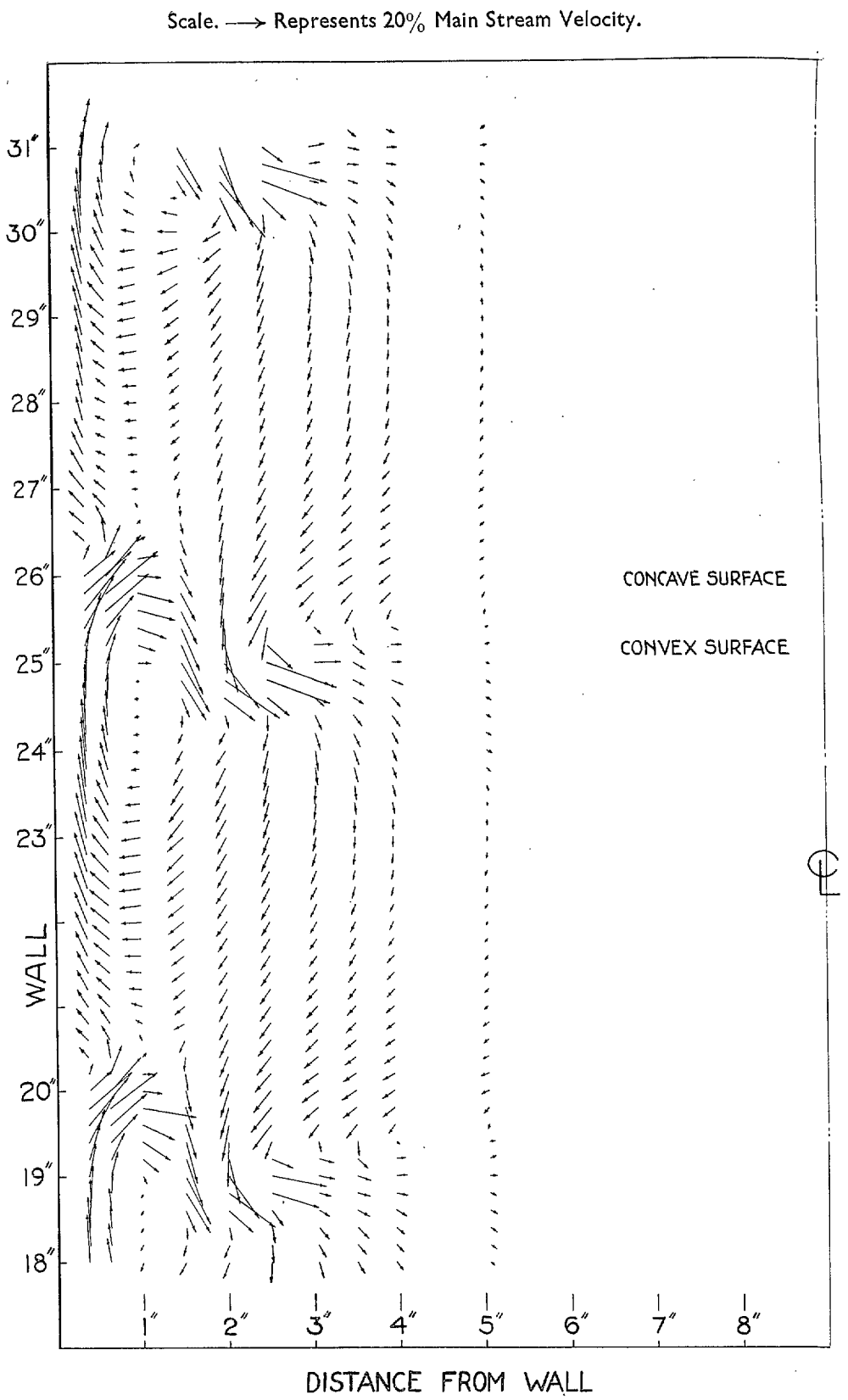


FIG. 8. Turbine blade cascade induced velocity vectors in a plane $\frac{1}{2}$ chord downstream of trailing edge. Thin upstream boundary layer.

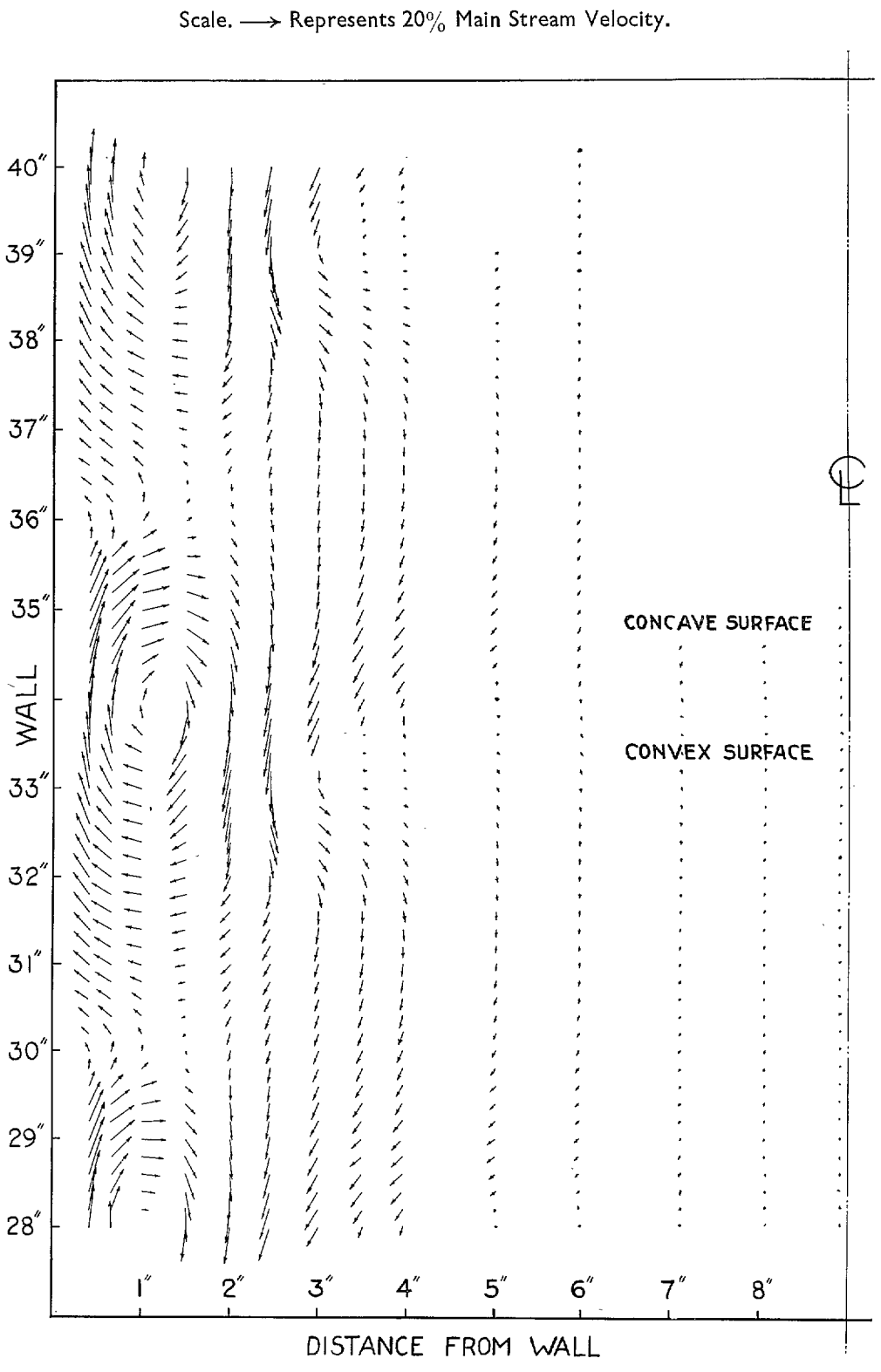


FIG. 9. Turbine blade cascade : induced velocity vectors in a plane $1\frac{1}{2}$ chords downstream of trailing edge. Thin upstream boundary layer.

J4368 Wt.20/9036 K9 5/56 D&Co. 34/263



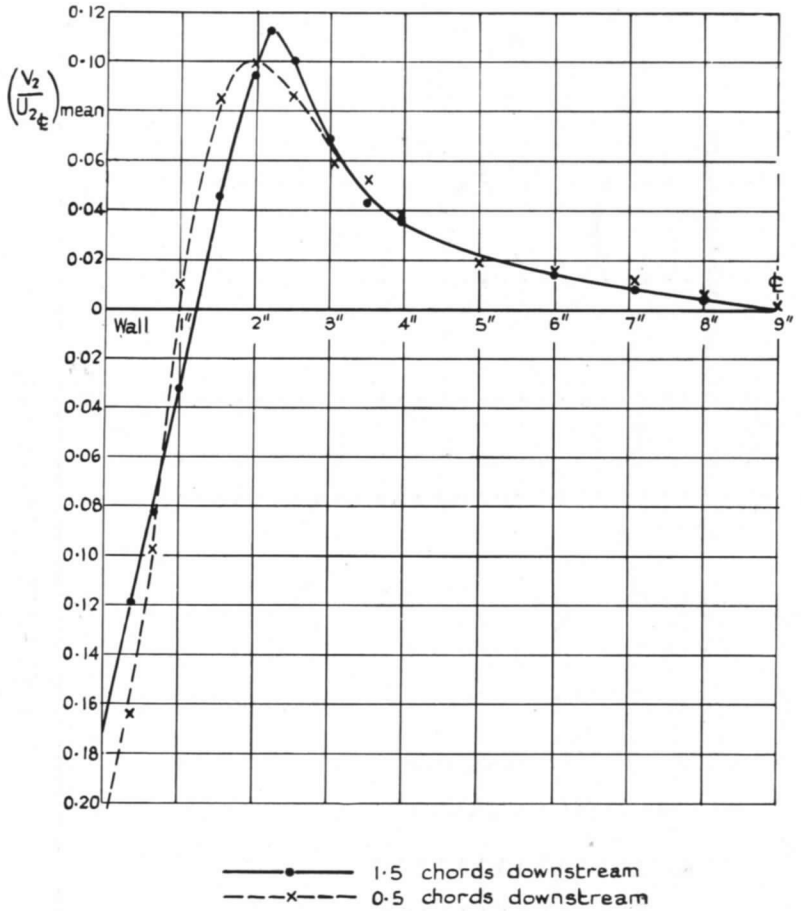


FIG. 10. Mean induced velocity $V_2$. Thin boundary layer.

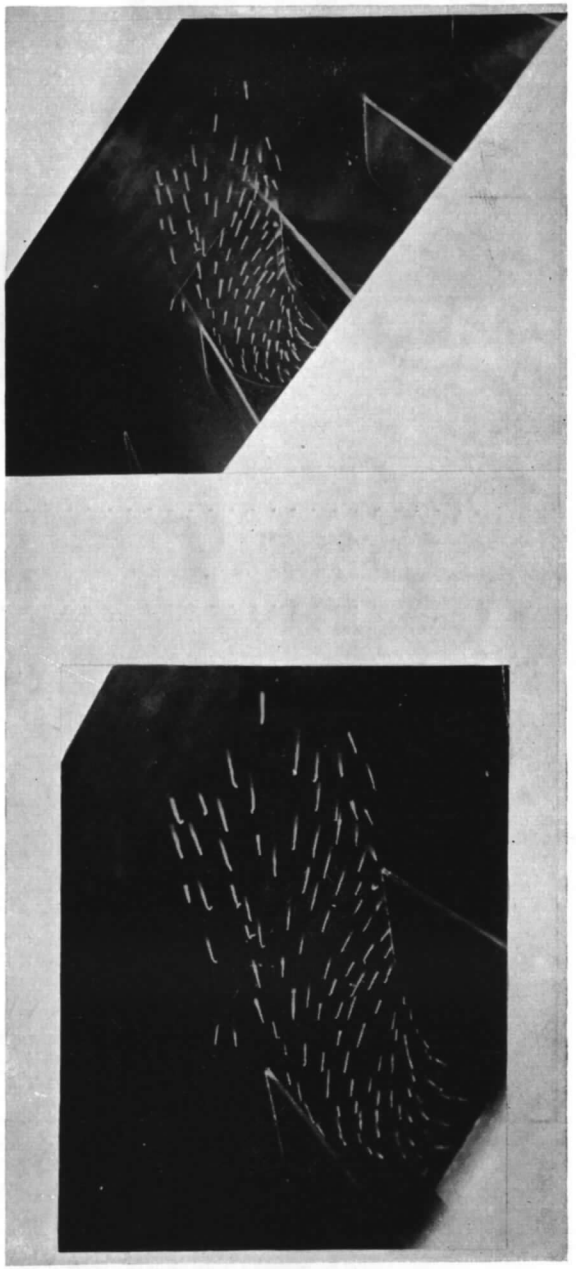

FIG. 11. Photographs of goosedown tufts.

PRINTED IN GREAT BRITAIN

# Publications of the Aeronautical Research Council

## ANNUAL TECHNICAL REPORTS OF THE AERONAUTICAL RESEARCH COUNCIL (BOUND VOLUMES)

1939 Vol. I. Aerodynamics General, Performance, Airscrews, Engines. 50*s.* (51*s.* 9*d.*)
Vol. II. Stability and Control, Flutter and Vibration, Instruments, Structures, Seaplanes, etc. 63*s.* (64*s.* 9*d.*)

1940 Aero and Hydrodynamics, Aerofoils, Airscrews, Engines, Flutter, Icing, Stability and Control, Structures, and a miscellaneous section. 50*s.* (51*s.* 9*d.*)

1941 Aero and Hydrodynamics, Aerofoils, Airscrews, Engines, Flutter, Stability and Control, Structures. 63*s.* (64*s.* 9*d.*)

1942 Vol. I. Aero and Hydrodynamics, Aerofoils, Airscrews, Engines. 75*s.* (76*s.* 9*d.*)
Vol. II. Noise, Parachutes, Stability and Control, Structures, Vibration, Wind Tunnels. 47*s.* 6*d.* (49*s.* 3*d.*)

1943 Vol. I. Aerodynamics, Aerofoils, Airscrews. 80*s.* (81*s.* 9*d.*)
Vol. II. Engines, Flutter, Materials, Parachutes, Performance, Stability and Control, Structures. 90*s.* (92*s.* 6*d.*)

1944 Vol. I. Aero and Hydrodynamics, Aerofoils, Aircraft, Airscrews, Controls. 84*s.* (86*s.* 3*d.*)
Vol. II. Flutter and Vibration, Materials, Miscellaneous, Navigation, Parachutes, Performance, Plates and Panels, Stability, Structures, Test Equipment, Wind Tunnels. 84*s.* (86*s.* 3*d.*)

1945 Vol. I. Aero and Hydrodynamics, Aerofoils. 130*s.* (132*s.* 6*d.*)
Vol. II. Aircraft, Airscrews, Controls. 130*s.* (132*s.* 6*d.*)
Vol. III. Flutter and Vibration, Instruments, Miscellaneous, Parachutes, Plates and Panels, Propulsion. 130*s* (132*s.* 3*d.*)
Vol. IV. Stability, Structures, Wind tunnels, Wind Tunnel Technique. 130*s.* (132*s.* 3*d.*)

## ANNUAL REPORTS OF THE AERONAUTICAL RESEARCH COUNCIL—

1937 2*s.* (2*s.* 2*d.*) 1938 1*s.* 6*d.* (1*s.* 8*d.*) 1939–48 3*s.* (3*s.* 3*d.*)

## INDEX TO ALL REPORTS AND MEMORANDA PUBLISHED IN THE ANNUAL TECHNICAL REPORTS, AND SEPARATELY—

April, 1950 – – – – – R. & M. No. 2600. 2*s.* 6*d.* (2*s.* 8*d.*)

## AUTHOR INDEX TO ALL REPORTS AND MEMORANDA OF THE AERONAUTICAL RESEARCH COUNCIL—

1909–January, 1954 – – – R. & M. No. 2570. 15*s.* (15*s.* 6*d.*)

## INDEXES TO THE TECHNICAL REPORTS OF THE AERONAUTICAL RESEARCH COUNCIL—

December 1, 1936 — June 30, 1939. R. & M. No. 1850. 1*s.* 3*d.* (1*s.* 5*d.*)
July 1, 1939 — June 30, 1945. – R. & M. No. 1950. 1*s.* (1*s.* 2*d.*)
July 1, 1945 — June 30, 1946. – R. & M. No. 2050. 1*s.* (1*s.* 2*d.*)
July 1, 1946 — December 31, 1946. R. & M. No. 2150. 1*s.* 3*d.* (1*s.* 5*d.*)
January 1, 1947 — June 30, 1947. – R. & M. No. 2250. 1*s.* 3*d.* (1*s.* 5*d.*)

## PUBLISHED REPORTS AND MEMORANDA OF THE AERONAUTICAL RESEARCH COUNCIL—

Between Nos. 2251–2349. – – R. & M. No. 2350. 1*s.* 9*d.* (1*s.* 11*d.*)
Between Nos. 2351–2449. – – R. & M. No. 2450. 2*s.* (2*s.* 2*d.*)
Between Nos. 2451–2549. – – R. & M. No. 2550. 2*s.* 6*d.* (2*s.* 8*d.*)
Between Nos. 2551–2649. – – R. & M. No. 2650. 2*s.* 6*d.* (2*s.* 8*d.*)

*Prices in brackets include postage*

HER MAJESTY'S STATIONERY OFFICE

York House, Kingsway, London W.C.2; 423 Oxford Street, London W.1;
13a Castle Street, Edinburgh 2; 39 King Street, Manchester 2; 2 Edmund Street, Birmingham 3; 109 St. Mary Street, Cardiff; Tower Lane, Bristol 1; 80 Chichester Street, Belfast, *or through any bookseller*

S.O. Code No. 23-2979